International Journal of Pharmaceutics: X 5 (2023) 100185

Contents lists available at ScienceDirect

International Journal of Pharmaceutics: X

journal homepage: www.sciencedirect.com/journal/international-journal-of-pharmaceutics-x

Tackling acne vulgaris by fabrication of tazarotene-loaded essential oil-based microemulsion: *In vitro* and *in vivo* evaluation

Noha M. Badawi [a,*], Rania M. Yehia [a], Caroline Lamie [a], Khaled A. Abdelrahman [b], Dalia A. Attia [a], Doaa A. Helal [c]

[a] Department of Pharmaceutics and Pharmaceutical Technology, Faculty of Pharmacy, The British University in Egypt, Cairo, Egypt
[b] Department of Microbiology, Faculty of Pharmacy, The British University in Egypt, Cairo, Egypt
[c] Department of Pharmaceutics, Faculty of Pharmacy, Fayoum University, Fayoum 63514, Egypt

ARTICLE INFO

Keywords:
Tazarotene
Microemulsion
Jasmine oil
Jojoba oil
Ex vivo skin deposition
P. acnes
Ear-infected acne mice model

ABSTRACT

This study aimed to formulate and optimize an anti-acne drug namely tazarotene (TZR) in essential oil-based microemulsion (ME) using either Jasmine oil (Jas) or Jojoba oil (Joj). TZR-MEs were prepared using two experimental designs (Simplex Lattice Design®) and characterized for droplet size, polydispersity index, and viscosity. Further *in vitro*, *ex vivo,* and *in vivo* investigations were performed for the selected formulations. Results revealed that TZR-selected MEs exhibited suitable droplet size, homogenous dispersions, and acceptable viscosity, in addition to spherical-shaped particles in morphology. The *ex vivo* skin deposition study showed a significant TZR accumulation in all skin layers for the Jas-selected ME over the Joj one. Further, TZR didn't show any antimicrobial activity against *P. acnes*, however, it was boosted when it was incorporated into the selected MEs. The *in vivo* study results of the infected mice ears induced by *P. acnes* revealed that our selected MEs successfully reached a high level of ear thickness reduction of 67.1% and 47.4% for Jas and Joj selected MEs, respectively, *versus* only 4% for the market product. Finally, the findings confirmed the ability to use essential oil-based ME, particularly with Jas, as a promising carrier for topical TZR delivery in the treatment of acne vulgaris.

1. Introduction

Acne vulgaris is a prevalent, long-lasting, inflammatory disease of the pilosebaceous unit that typically appears during puberty but can arise at any age, particularly in women. It is related to a variety of clinical manifestations, including comedones, nodules, papules, and pustules (Mohiuddin, 2019). The pathophysiology consists of four main factors that interact to cause acne lesions namely, androgen-dependent hyper-seborrhea, abnormal follicular keratinization leading to comedones, follicular colonization by *Propionibacterium acnes (P. acnes)*, and inflammatory mediators that are released in the skin (Taylor et al., 2011). Acne lesions frequently appeared on the areas with the most sebaceous glands, for example, the face, neck, upper chest, shoulders, and back (Williams et al., 2012). Treatment options for acne include topical, systemic, and other procedures such as chemical peeling and autografting. For mild to moderate acne, topical therapy is the initial line of defense against the condition. It has several benefits, including increased exposure to pilosebaceous units and less systemic absorption (Fox et al., 2016). However, the majority of topical formulations frequently cause adverse effects such as skin irritability, erythema, and itch, which reduce both patient compliance and therapeutic effectiveness (Sevimli Dikicier, 2019). Therefore, delivering highly efficient and well-tolerated therapy is the definitive goal concerning topical acne treatment (Katsambas and Dessinioti, 2008; Otlewska et al., 2020).

Tazarotene (TZR), which belongs to a new class of receptor-selective synthetic retinoids, is a 6-[2-(4,4-dimethylthiochroman- 6-yl)ethyn2yl] nicotinic acid ethyl ester used topically to treat acne vulgaris (Patel et al., 2016). TZR is a retinoid prodrug that is transformed in the skin by de-esterification to tazarotenic acid which is its active metabolite. Tazarotenic acid binds to all three members of the retinoic acid receptor (RAR) family – RARα, RARβ, and RARγ, but displays a relative preference for RARβ and RARγ (Gregoriou et al., 2014). The RARγ is primarily found in the epidermis, while the RARβ is primarily found in fibroblasts. The TZR active moiety forms a complex with the RAR that afterward binds to the retinoid X receptor (RXR), which controls gene transcription by binding to particular DNA sites, hindering cell proliferation while

* Corresponding author at: The British University in Egypt, El Sherouk City, Suez Desert Road, Cairo, P.O. Box 11562, Egypt.
E-mail address: Noha.Alaa@bue.edu.eg (N.M. Badawi).

https://doi.org/10.1016/j.ijpx.2023.100185
Received 18 March 2023; Received in revised form 23 May 2023; Accepted 26 May 2023
Available online 29 May 2023

also regulating cell differentiation and the inflammatory process (Yehia et al., 2022). It was stated that the basis of the therapeutic effect of TZR in acne is possibly a result of its anti-hyperproliferative, normalizing of differentiation, along with its anti-inflammatory properties (Gregoriou et al., 2014). Though, it has some drawbacks including skin irritation in addition to its poor solubility. To combat these adverse effects and improve its topical therapeutic potential in acne treatment, an effective carrier system for TZR better to be developed (Nasr et al., 2017).

Nanocarriers have several benefits for topical drug delivery, including improved skin availability, greater penetration, and functioning as a depot to extend dermal drug release (Nasr et al., 2017). Microemulsions (MEs) are among the promising non-vesicular nanocarriers, which are primarily suggested for enhancing percutaneous drug permeation. MEs are thermodynamically stable, homogenous, transparent, and isotropic colloidal dispersions with mean droplet sizes ranging from 10 to 200 nm. It consists of two immiscible liquids (oil and water) held together by an interfacial monomolecular film of a surfactant or mixtures of surfactants, usually combined with a cosurfactant to be stabilized (Vlaia et al., 2022; Yehia and Attia, 2019). Various studies proved that MEs can provide extended drug release, reduce the drug's skin irritation effect and shield the encapsulated drug from degradation (Lawrence and Rees, 2000; Nastiti et al., 2017). In addition, the oily portion of the MEs may consist of essential oils (EOs) which are considered a new type of skin penetration enhancers of natural origin since they are not only highly potent (Das and Gupta, 2021; Fox et al., 2011; Herman and Herman, 2015), but also safe, reported in the FDA's list of generally recognized as safe (GRAS) agents (Vostinaru et al., 2020). Furthermore, many previous studies have shown that EOs, as complex mixtures of a variety of volatile and non-volatile compounds, have extensive antimicrobial activity against a wide range of microorganisms, including viruses, bacteria, and fungi (Figueiredo, 2017; León-Méndez et al., 2019; Nazzaro et al., 2017).

We hypothesized that EO-based ME as a delivery system for TZR could evoke a synergistic strategy to produce a potential candidate for the treatment of acne. Therefore, our study's goal was to formulate TZR in an EO-based ME to take advantage of the carrier system's nanosize and surfactant/cosurfactant content to achieve better TZR deposition into the skin for enhanced efficacy. In addition, use ME to counteract TZR's irritant nature; minimize the transdermal delivery of this drug, and improve its topical localization by using optimal formulations *via* simplex lattice design®. Furthermore, we studied the antimicrobial activity of the selected MEs *in vitro* against *P.acnes* in comparison to the Free TZR. In addition, the antiacne effect for the optimized ME formulations was compared *in vivo* using the ear-infected acne mice model.

2. Materials and methods

2.1. Materials

Tarazotene (TZR) was obtained on gratis from Dr. Reddy's Laboratory Ltd., (Andhra Pradesh, India). Capryol 90, Labrafac CC, Labrafil M, Labrafac PG, Labrasol, Transcutol, and Plurol oleique were obtained as a gift sample from (Gattefossè, Saint-Priest, France); Propylene glycol, Span 80 and Tween 80 were purchased from El-Nasr Pharmaceutical Chemicals (Abu Zaabal, Egypt). All other chemicals and solvents were of pure analytical grade.

2.2. Methods

2.2.1. Screening of TZR solubility in several EOs

Preliminary investigations were conducted to identify oils that provide high drug solubility. The TZR's saturation solubility in the inspected EOs (Tea tree, Jasmine, Jojoba, Green tea, and Rosemary) was determined in triplicate. TZR was added with an excess amount to each sealed glass vial containing 1 mL of the chosen EOs and shaken for 72 h at room temperature in a thermostatically controlled shaker water bath (Julabo SW-20C, Allentown, PA) till equilibrium. Subsequently, centrifugation (Centurion SCI, West Sussex, UK) was done for the resulting dispersion at 15,000 rpm for 10 min then supernatant filtration through a Millipore membrane filter (0.45 μm) was performed. Afterward, ethanol was used to dilute a half gram of the filtrate, and the absorbance of this filtrate was then examined spectrophotometrically (spectrophotometer UV 1601, PC UV–visible, Shimadzu, Kyoto, Japan) at the wavelength of the predetermined wavelength of maximum absorbance (λ_{max}) 347 nm against a blank which consists of the same oil in ethanol with equal dilution factor (Hashem et al., 2011), and the concentration of TZR was calculated utilizing a pre-constructed calibration curve (Radwan et al., 2017).

2.2.2. Construction of pseudo-ternary phase diagrams

The pseudo-ternary phase diagrams were created *via* the water titration method using the selected EOs (Yehia et al., 2017). First, the mixing of the oily phase and a mixture of surfactant and cosurfactant was performed in ratios from 1:9 to 9:1 in glass vials at room temperature. The drug (TZR 0.1%) was dissolved in the oily phase. After settling, mixtures were classified visually as either two-phase or multiple-phase MEs. Turbidity was considered a sign of phase separation (Yehia et al., 2017). Each component weight percent in the ternary phase system was determined, and the pseudo-ternary phase diagrams were created by plotting the phase diagrams on triangular coordinates using TriDraw software version 4.5. The Supplementary material: Table S1 displays the composition of the prepared systems.

2.2.3. Optimization of ME formulations according to simplex lattice mixture

2.2.3.1. Experimental design. Optimization of the selected ME systems was done using the simplex lattice design® using the Design-Expert 11 program (Stat-Ease, Inc., Minneapolis, MN, USA). Three components in the ME, including the weight percent of oily phase (X1), weight percent of water (X2), and weight percent of surfactant/ cosurfactant (X3), were nominated as independent factors. While, the droplet size (nm) (Y1), polydispersity index (PDI) (Y2,) and viscosity (cP) (Y3) were the chosen responses. In the simplex lattice design®, the feasible experimental region was the largest triangular shape under the ME region. The ME system components were investigated by simultaneously changing their concentrations, and the three components total concentration was set to 100%. The MEs were prepared using the formulations in the pseudo-ternary phase diagrams provided by the design under the ME regions. All components were precisely weighed and mixed carefully. The resultant MEs were kept in closed containers at room temperature, prior to further assessments (Duangjit et al., 2014).

2.2.4. Characterization of ME formulations

2.2.4.1. Droplet size, and polydispersity index (PDI) determination. The mean droplet size and PDI were measured by dynamic light scattering (DLS) without dilution by Zetasizer (ZEN 3600, Malvern Instruments, UK). The fluctuations in light scattering due to the Brownian motion of particles were observed at 25 °C at a 90° angle (Yehia et al., 2017). All determinations were made in triplicate and the mean ± SD was reported.

2.2.4.2. Viscosity measurement. Viscosity was measured to all prepared MEs at room temperature with a Brookfield viscometer (DV-III+ Pro Brookfield, USA) using spindle no. 52 with a shear rate of 100 rpm. Each measurement was carried out three times and the mean ± SD was deduced (Nasr and Abdel-Hamid, 2016).

2.2.4.3. Electrical conductivity measurement. The electrical conductivities of the prepared MEs were assessed using a conductivity meter (S230

Seven Compact™, Mettler Toledo, Switzerland), Each assessment was performed in triplicate and the mean ± SD was calculated (Kizibash et al., 2011).

2.2.4.4. Morphological evaluation. The morphological investigation of the optimum MEs was done *via* a transmission electron microscope (TEM) (model JEM-1230, JEOL, Tokyo, Japan), operating at 80 kV. On the surface of a carbon-coated copper grid one drop of the ME was placed, after being negatively stained with 1% phosphotungstic acid, and then left to be dried for 10 min at room temperature before being investigated (Nasr and Abdel-Hamid, 2016).

2.2.4.5. Ex vivo skin deposition studies. The optimum MEs *ex vivo* skin deposition investigations were examined *via* Franz diffusion cell with a receptor chamber with a volume of 12.5 mL using Swiss albino mice's abdominal skin as a dialyzing membrane (Bachhav and Patravale, 2009; Nasr et al., 2017). After equilibration in phosphate buffer solution pH 7.4 (PBS) for 4 h, the skin membranes were placed between the receptor and donor compartments, in the Franz-diffusion cell, with the dermal side facing the former. To ensure sink conditions by increasing the solubility of TZR in the receiving phase, 12 mL of PBS: Ethanol (7:3 *v*/v) was added to the receptor chamber. The entire assembly was set up in a thermostatically controlled water bath stirred at 100 rpm and kept at a temperature of 37 °C ± 0.5 °C. The donor compartment, which has a diffusion area of 1.77 cm^2, was filled with a precisely weighed amount of the selected ME formulations. After 24 h, samples were taken from the receptor compartment and to get rid of the un-permeated drug/formula, the top layer of the skin was rinsed five times using distilled water. To measure TZR deposited amounts in each skin layer, the tape stripping method was applied. First, the stratum corneum was separated by stripping the skin twenty times using adhesive tape. Afterward, the dermis was detached from the epidermis by scalpel peeling. Then to ensure complete extraction of the TZR, each skin layer was sonicated with ethanol for 6 h (Lamie et al., 2022). All samples were analyzed spectrophotometrically at 374 nm including samples from the receptor compartment and compared to a blank (without drug) to avoid any interference. Moreover, Jas and Joj solutions of TZR (0.1%) were used as control. All measurements were done in triplicate and the mean ± SD was calculated.

2.2.4.6. Qualitative tracing of the fluorescently labeled selected MEs using confocal laser scanning microscopy (CLSM). Dil fluorescent dye was selected as the model tracer for the visualization of the transcutaneous pathway following the topical application of the selected MEs using confocal laser microscopy (Zeiss LSM 710, Germany coupled with ZEN 2009 software, excitation wavelength: 543 nm, emission wavelength: 633 nm). TZR loaded into the selected MEs was partially replaced by the Dil fluorescent dye, implementing the same preparation method described previously to obtain the fluorescently labeled formulae. As previously explained in the quantitative *ex vivo* deposition study those labeled formulae were mounted on the donor compartment of the Franz diffusion cell for 24 h, then, the skin sections were detached from the diffusion cells, washed, and stored for further manipulations required for optical imaging (Lamie et al., 2022). The results were analyzed using GraphPad Prism 8 software (San Diego, CA, USA) using two-way ANOVA, followed by Sidak's multiple comparisons *post hoc* test, and $p < 0.05$ was considered significant.

2.2.5. Antimicrobial activity assay

The antibacterial activity of TZR, either free or in MEs formulae, was tested against *P. acnes* (ATCC 6919) at various concentrations *versus* the respective control. The bacteria were cultivated for 48–72 h at 37 °C on reinforced clostridial medium (RCM) agar. Each well in a 96-well plate received 100 µL of RCM broth. In the first well, 100 µL of each formulation dispersed in RCM broth was added and the drug suspension was serially diluted with RCM (2-fold dilution). Subsequently, the culture was diluted to 100-fold. Lastly, the *P. acnes* suspension adjusted to half McFarland (1 × 108 CFU/mL) was added to each well. Additionally, the plates were incubated at 37 °C under anaerobic conditions for 48 h. Then, the minimal inhibitory concentration (MIC) was calculated from the absorption measured spectrophotometry at 570 nm using a microplate reader (BioTek ELX800, USA) (Yehia et al., 2022). Each investigation was performed in triplicates.

2.2.6. In vivo evaluation using acne mice model

2.2.6.1. Animals and bacterial culture. Thirty-six male Balb/C mice weighing 20–30 g (obtained in-house) were used in the current study. The animals were randomized and kept under a temperature of 22 ± 3 °C, 5% humidity, and 12 h light/dark, with free access to standard laboratory food and water. The study was conducted according to the Helsinki agreement protocol and the regulations of the 'Guide for the Care and Use of Laboratory Animals and the requirements of the research ethics committee for experimental and clinical studies at the Faculty of Pharmacy, The British University in Egypt (no. EX-2205). In addition, standard *P. acnes* strain ATCC 6919 was grown under anaerobic conditions on RCM broth for 48 h at 37 °C. The bacterial suspension was used for the preparation of the inoculum (Abdelhamed et al., 2022).

2.2.6.2. Experimental design. The induction of inflammatory acne in a mouse model was done by injecting the right-side ears of Balb/C mice intra-dermally with 1.0×10^7 CFU per 20 µL in saline of living *P. acnes*. Mice left side ears were uninfected. After 24 h microcomedone formation was observed visually and an increase in ear thickness by an average of 0.1 mm as measured by Vernier caliper (Luo et al., 2021). The mice's uninfected left ear served as a control group; Group A. Mice were then divided into four groups ($n = 6$ mice/group). Group B acted as the model group receiving no treatment. Group C mice received treatment with market gel product containing 0.1% TZR (0.1 g gel twice daily). Groups D and E mice received treatment with the optimized EO-ME formulations containing 0.1% TZR (100 µL ME twice daily). Each infected right-side mice ear of the treatment groups received the doses by applying a thin film of the selected formulation epicutaneously. The treatment lasted for 3 consecutive days with a total of 5 doses applied. The sizes of the microcomedones - like cysts of all groups were measured daily by calculating the difference between the infected ear sizes and the uninfected ones using a Vernier caliper. Each measurement was performed in triplicates. Moreover, digital photographs were taken on daily bases prior and post treatment to monitor the inflammation progress (Abdelhamed et al., 2022).

2.2.6.3. Statistical analysis. The differences between the mean values of the uninfected ears and the infected ones for each group were assessed with a two-way analysis of variance ANOVA followed by Tukey's multiple comparison test using GraphPad Prism version 13.0 (GraphPad Software, San Diego, CA, USA) to examine the effect of the applied gels on induced acne. Values of $P < 0.05$ were considered significant.

2.2.6.4. Histopathological evaluation. After receiving topical treatment for three days, mice were mercifully sacrificed and the infected ears for treatment groups as well as the model group along with the control group (normal uninfected ears) were dissected and stored in 10% neutral formalin for around 72 h. The organs' samples were then treated with ethanol and xylene and infiltrated with synthetic paraplast tissue embedding medium. Rotatory microtome was utilized to cut the tissue sections at the middle zones of different auricular samples for demonstration of different skin layers. Subsequently, tissues were fixed onto slides and stained by hematoxylin and eosin (H&E stain) then examined blindly by a qualified histologist and imagery using a Full HD microscopic imaging system (Leica, Germany) (Abdelhamed et al., 2022).

3. Results and discussion

3.1. Screening of TZR solubility in various oils

In order to identify the oils with the greatest ability to solubilize TZR, a solubility study was conducted, which will lead to a bigger ME area in the pseudo-ternary plots (Khichariya et al., 2022). The choice of oil in ME is a crucial stage since it influences the size of the globules, the amount of drug loaded, and the amount of surfactant/cosurfactant needed to create a stable ME (Khichariya et al., 2022). Fig. 1 illustrated the solubility data for TZR in various EOs. Jasmine essential oil (Jas) (30.22 ± 0.34 mg/mL) followed by Jojoba essential oil (Joj) (28.16 ± 1.12 mg/mL) demonstrated the highest level of TZR solubility among other oils. This may be attributed to the concept of like dissolves like and due to TZR being a very lipophilic drug (Log $P = 5.96$) so it will be more soluble in the oils with the highest lipophilicity (Nasr and Abdel-Hamid, 2016). Consequently, Jas and Joj provided superior solubility for TZR based on the degree of lipophilicity of the used oils as described by their HLB values of 9, 5,6.5, 7, and 15 for Tea tree, Jasmine, Jojoba, Green tea, and Rosemary oils, respectively (Morais et al., 2008; Nasr and Abdel-Hamid, 2016; Putri et al., 2018; Rodríguez-Rojo et al., 2012).

3.2. Construction of pseudo-ternary phase diagrams

Various combinations of oily phase, surfactants, and cosurfactants were established to find the best combination that produced the largest ME domain. In the constructed pseudo-ternary phase diagrams, the ME systems containing either Jas or Joj as the oily phase as well as Tween 80, Span 80, and Labrasol as surfactant/cosurfactant demonstrated the largest ME regions. Accordingly, the S12 systems with either Jas or Joj were chosen for further optimization studies. In addition, Tween 80 because of its large head group allowed it to pack more loosely at the interface and effectively integrate oil chains into surfactant tails, making it an ideal surfactant for our system (Nasr and Abdel-Hamid, 2016). Additionally, the addition of Span 80 to our system lowers the HLB values of Tween 80 and Labrasol, allowing Jas and Joj to successfully penetrate their hydrophobic zones. This results in the production of MEs with a wider range of compositions (Nasr and Abdel-Hamid, 2016). Fig. 2 demonstrated the pseudo-ternary phase diagrams of the chosen systems.

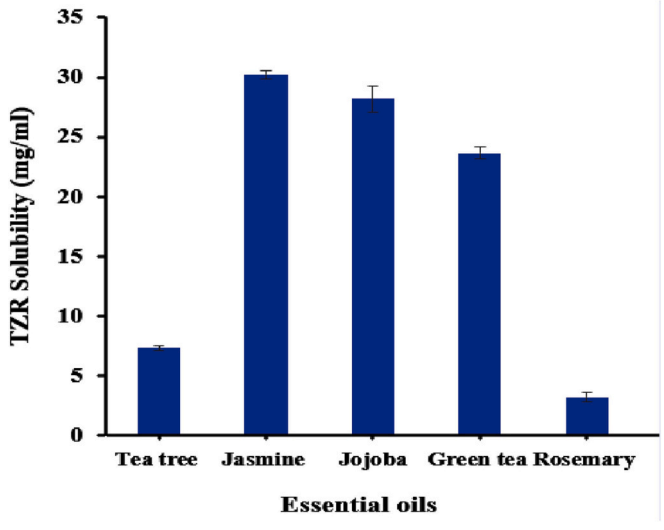

Fig. 1. Solubility study of TZR in various EOs.

3.3. Optimization of ME formulations according to simplex lattice mixture experimental design

Simplex lattice design® was applied to test the effect of the independent variables on the dependent ones. The selected ranges for several components of the independent variables were as follows: X1–oil (8–39%), X2–water (1–32%), and X3– surfactant/ cosurfactant (60–91%). While, the chosen response variables were the droplet size (Y1), the PDI (Y2), and the viscosity (Y3). Two separate designs were applied for both Jas and Joj. The developed designs proposed 12 experimental runs for each, representing all possible combinations of the studied factors' different levels. Tables 1 and 2 showed the formulations' compositions as well as the results for systems of both Jas-ME and Joj-ME, respectively. Figs. 3 and 4 displayed the three-dimensional response surfaces and the contour plots generated from the simplex lattice design®.

3.3.1. Effect on the droplet size

For the Jas system, the droplet size ranges from 8.96 ± 1.9 to 669.55 ± 21.4 nm (Table 1). The generated quadratic model was significant at $P < 0.05$. The model's adequate precision in measuring the signal-to-noise ratio was 9.9, indicating an adequate signal. A ratio >4 is usually preferred. Furthermore, the predicted R-Squared of 0.9163 was in good harmony with the adjusted R-Squared of 0.8326, indicating the model's high predicting capability. It was observed in the Jas-ME formulations that upon increasing the surfactant amount the droplet size increases. This may be attributed to the produced aggregates in the continuous phase due to excess surfactant molecules, which decreases the surfactant concentration available to cover the oil phase. As a result, the size of the droplets would rise. In addition, excess surfactant could also result in depletion in the flocculation (Sarheed et al., 2020). On the other hand, the droplet size ranges from 17.49 ± 3.83 to 736.7 ± 57.28 nm for the Joj system (Table 2). The created quadratic model was also significant at $P < 0.05$ with an adequate precision value of 19.3. The predicted R-Squared as well as the adjusted R-Squared were 0.9845 and 0.9690, respectively. It was detected that, upon increasing the oil amount the droplet size increases in the Joj-ME formulations. It was stated before, oils with a high concentration of polar compounds reduce the interfacial tension and enable droplet disruption during homogenization. In our case, Joj is a simple ester that was esterified to a fatty acid alcohol (Shevachman et al., 2004), thus providing high polarity which in turn led to a decrease in the interfacial tension resulting in a smaller particle size (Sarheed et al., 2020).

3.3.2. Effect on the polydispersity index

The polydispersity index (PDI) varied between 0.21 ± 0.0007 and 1 ± 0 for the Jas design (Table 1). The model generated was the special quadratic model which is more suitable for modelling multicomponent mixtures data and can be utilized to evaluate multiple effects as well as the curvature of a response surface in the interior of a triangle in order to generate contour-like effects (Mazonde et al., 2020). The model was significant at $P < 0.05$ with adequate precision, predicted, and adjusted R-Squared of 60.8, 1.0000, and 1.0000, respectively. The lowest PDI values were found to be in the center of the triangle with an average % of all independent variables. Large PDI value could be attributed to the presence of bicontinuous structure ME (Hathout and Elshafeey, 2012) and also may be due to destabilization processes such as coalescence or Ostwald ripening that may occur due to the specific composition of oil and surfactant (Yuliani and Noveriza, 2019). Alternatively, for the Joj design, the PDI values ranged from 0.161 ± 0.0064 to 1 ± 0 (Table 2). The special quadratic model was also significant at $P < 0.05$ with predicted and adjusted R-Squared of 0.9905 and 0.9525, respectively as well as the adequate precision was 15.8. It was found that upon increasing the water amount the PDI values decrease. This could be due to that higher water concentration reduces viscosity and facilitate the formation of uniform particles (Butt et al., 2016).

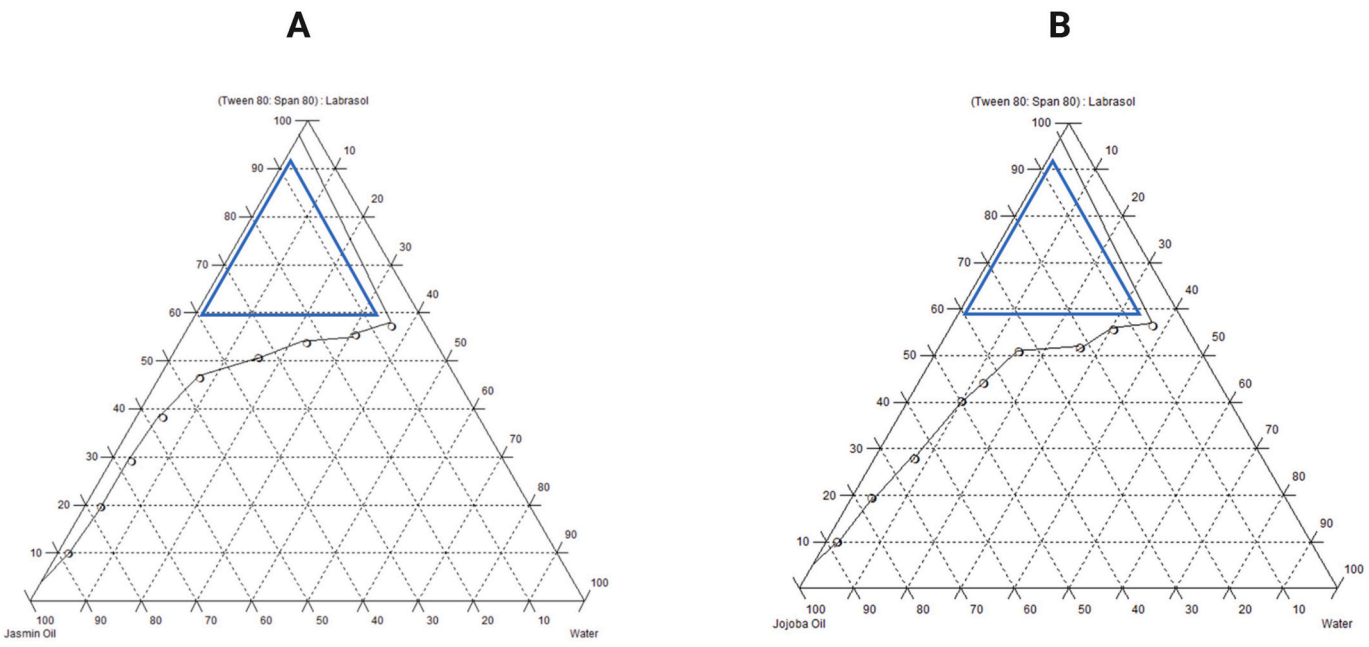

Fig. 2. Pseudo-ternary phase diagrams of the selected ME systems: (A) Jas / (Span80, Tween80), Labrasol 1:1:2 / Water system, (B) Joj / (Span80, Tween80), Labrasol 1:1:2 / Water system. The triangular shapes boarder the Simplex lattice design®.

Table 1
Formulations, compositions, and results of TZR loaded Jas-MEs.

Formula no.	Oil %	Water %	SAA mix[a] %	Droplet size (nm)	PDI	Viscosity (cP)	Conductivity (μS/cm)
1	39	1.0	60.0	78.84 ± 0.90	1.00 ± 0.00	490 ± 7	0.13 ± 0.01
2	28.7	6.2	65.2	29.69 ± 1.70	0.25 ± 0.00	390 ± 14	3.64 ± 0.05
3	18.3	11.3	70.3	15.30 ± 0.30	0.21 ± 0.00	300 ± 14	3.58 ± 0.12
4	13.2	6.2	80.7	19.70 ± 0.10	0.58 ± 0.16	260 ± 2	1.89 ± 0.07
5	8	32.0	60.0	31.43 ± 0.30	0.99 ± 0.01	200 ± 12	37.20 ± 1.30
6	8	32.0	60.0	22.76 ± 8.50	1.00 ± 0.00	200 ± 3	39.10 ± 0.98
7	8	1.0	91.0	579.50 ± 35.60	1.00 ± 0.00	210 ± 15	0.79 ± 0.06
8	23.5	16.5	60.0	22.19 ± 6.40	0.67 ± 0.27	350 ± 18	12.91 ± 0.07
9	13.2	21.7	65.2	8.96 ± 1.90	0.30 ± 0.07	290 ± 11	21.60 ± 1.10
10	39	1.0	60.0	669.55 ± 21.40	1.00 ± 0.00	500 ± 10	0.37 ± 0.02
11	8	16.5	75.5	14.26 ± 0.10	0.48 ± 0.06	205 ± 14	9.56 ± 0.08
12	23.5	1.0	75.5	65.90 ± 14.30	0.75 ± 0.15	350 ± 18	0.59 ± 0.03

Abbreviations: SAA mix; surfactant mixture, PDI; polydispersity index.
Notes: Results are expressed as the mean of three replicates ± SD.
All formulations were prepared with TZR 0.1% (1 mg/mL).
X1; Oil, X2; Water, X3; surfactant/ cosurfactant, Y1; Droplet size, Y2; PDI, Y3; Viscosity.
[a] SAA mixture; (Span80, Tween80), Labrasol 1:1:2.

Table 2
Formulations, compositions, and results of TZR loaded Joj-MEs.

Formula no.	Oil[a] %	Water %	SAA mix %	Droplet size (nm)	PDI	Viscosity (cP)	Conductivity (μS/cm)
1	29.3	6.3	64.3	41.38 ± 3.49	0.38 ± 0.06	750 ± 7	1.42 ± 0.05
2	8	1	91	155.30 ± 27.26	0.79 ± 0.14	458 ± 6	1.26 ± 0.23
3	13.3	6.3	80.3	51.92 ± 5.88	1.00 ± 0.00	600 ± 7	1.74 ± 0.03
4	8	33	59	130.00 ± 10.35	1.00 ± 0.00	360 ± 2	38.30 ± 1.20
5	8	33	59	123.00 ± 13.26	0.93 ± 0.12	375 ± 5	39.20 ± 1.40
6	18.7	11.7	69.7	27.66 ± 7.02	0.63 ± 0.26	523 ± 8	3.99 ± 1.20
7	40	1	59	736.70 ± 57.28	1.00 ± 0.00	800 ± 7	0.21 ± 0.02
8	13.3	22.3	64.3	17.49 ± 3.83	0.42 ± 0.22	473 ± 6	19.57 ± 0.80
9	8	17	75	18.82 ± 0.86	0.56 ± 0.03	530 ± 3	10.55 ± 0.45
10	40	1	59	619.00 ± 79.72	0.70 ± 0.00	820 ± 14	0.20 ± 0.02
11	24	1	75	500.00 ± 45.79	0.16 ± 0.01	433 ± 7	0.55 ± 0.10
12	24	17	59	18.69 ± 7.01	0.98 ± 0.03	435 ± 14	12.91 ± 0.08

Abbreviations: SAA mix; surfactant mixture, PDI; polydispersity index.
Notes: Results are expressed as the mean of three replicates ± SD.
All formulations were prepared with TZR 0.1% (1 mg/mL).
X1; Oil, X2; Water, X3; surfactant/ cosurfactant, Y1; Droplet size, Y2; PDI, Y3; Viscosity.
[a] Oily phase; Jojoba oil.

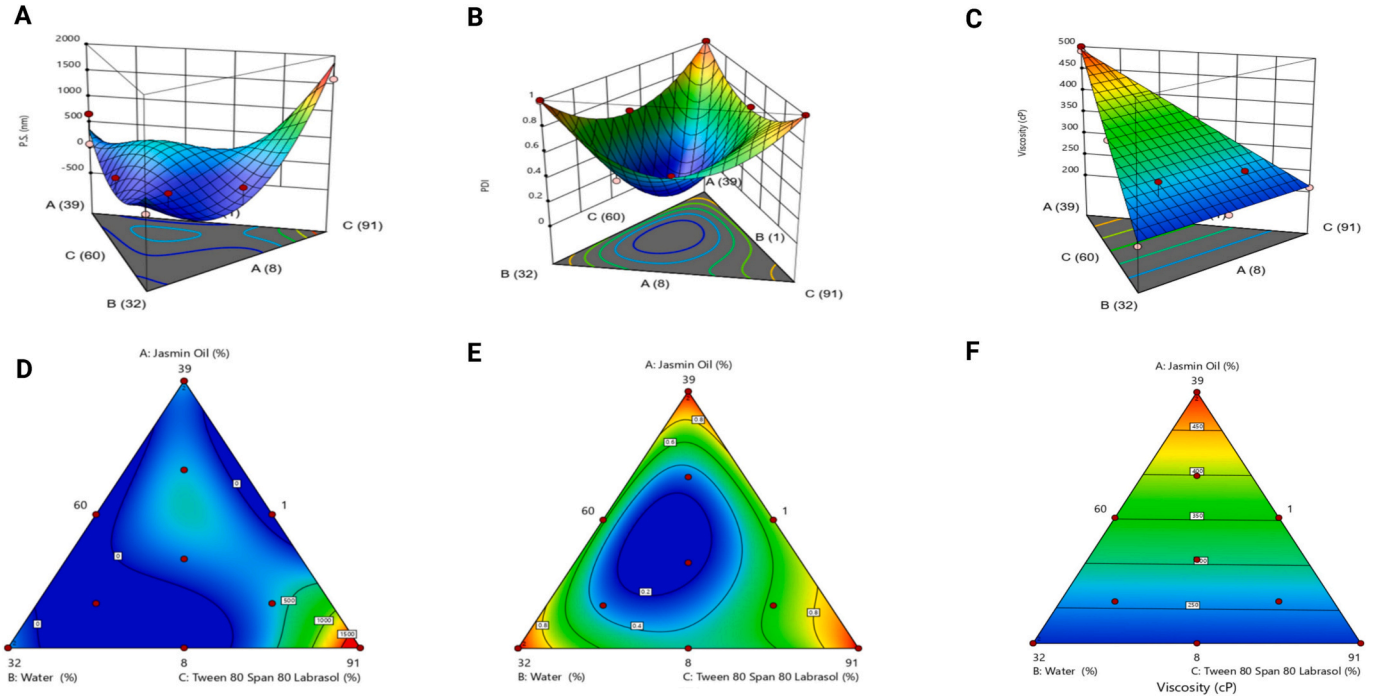

Fig. 3. Simplex lattice design® generated plots of (A, B, and C) three-dimensional response surfaces and (D, E, and F) contour plots of the responses namely droplet size, PDI, and viscosity, respectively, for the Jas-ME systems.

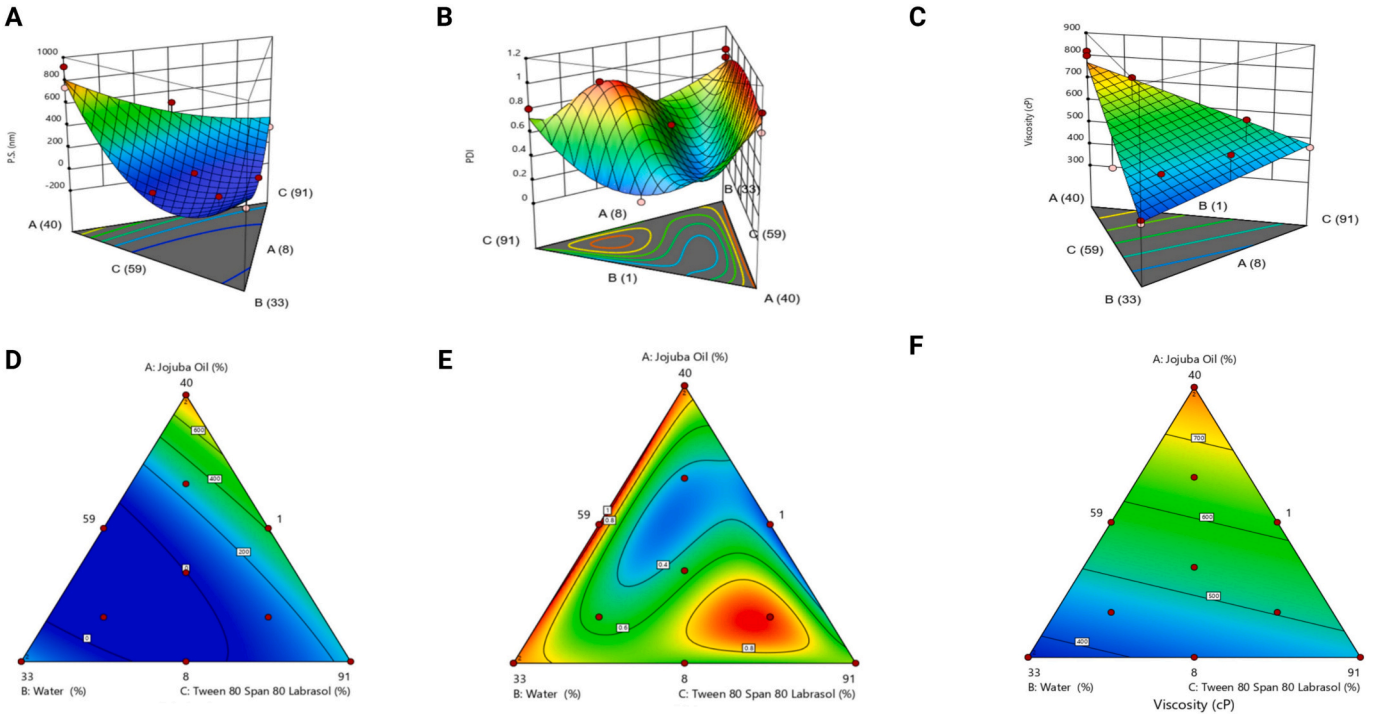

Fig. 4. Simplex lattice design® generated plots of (A, B, and C) three-dimensional response surfaces and (D, E, and F) contour plots of the responses namely droplet size, PDI, and viscosity, respectively, for the Joj-ME systems.

3.3.3. *Effect on the viscosity*

It was observed that linear significant models at $P < 0.05$ were created for both Jas and Joj designs. The adequate precision predicted and adjusted R-Squared were 12.5, 0.9909, and 0.9886, respectively, for Jas. While, for Joj they were 19.64, 0.8846, and 0.8557, respectively. The viscosity values ranged from 200 ± 3 to 500 ± 10 cP and from 360 ± 2 to 820 ± 14 cP for both Jas and Joj, respectively, as shown in Tables 1 and 2. Increasing the oil amount in both designs was found to have a positive effect on the viscosity which could be due to the high inherent viscosity of the oils and this result is in agreement with Thombre et al. (Thombre et al., 2022).

3.4. Electrical conductivity measurement

Electrical conductivity is a beneficial parameter for determining the type of ME. Three different types of MEs can exist theoretically: water-in-oil ME, bicontinuous ME, and oil-in-water ME. According to Djordjevic et al. evaluation for the ME type using electrical conductivity measurements (Djordjevic et al., 2004), water-in-oil ME was a formulation with a higher oil phase ratio than a lower water phase and conductivity between 2.9 and 3.8 μS/cm. MEs with a higher water-to-oil ratio and conductivities ranging from 10.3 to 52.5 μS/cm were classified as bicontinuous, whereas oil-in-water MEs had conductivities ranging from 80.5 to 94.3 μS/cm.

Since there have been no publications regarding the evaluation method for the type of MEs based on a cut-off value for electrical conductivity. Therefore, criteria were established based on the literature previously discussed in order to distinguish between different types of MEs utilizing both electrical conductivity and the ratio of the oil to water phases (Subongkot and Ngawhirunpat, 2017). It will be a water-in-oil ME if the ratio of the oil phase is greater than the water phase. It will be an oil-in-water ME if the ratio of the water phase to the oil phase is greater and the conductivity is >52.5 μS/cm. When the water phase to oil phase ratio is equal and the conductivity is not >52.5 μS/cm, the ME will be bicontinuous (Subongkot and Ngawhirunpat, 2017).

The conductivity of Jas-MEs ranged from 0.13 ± 0.01 to 39.1 ± 0.98 μS/cm whereas that of the Joj-MEs ranged from 0.2 ± 0.02 to 39.2 ± 0.4 μS/cm as shown in Tables 1 and 2, respectively, and Fig. 5. According to the above criteria, this suggested that both Jas and Joj fabricated MEs were water-in-oil or bicontinuous which is in harmony with the results of Subongkot et al. (Subongkot and Ngawhirunpat, 2017). It was also found that as the water content rises the electrical conductivity also rises which is reported before by Hathout et al. (Hathout et al., 2010). As shown in Fig. 5 the increase in the water percent was accompanied by the increase in the conductivity values and *vice versa* occurred in the case of the oil percent.

3.5. Optimization of formulation variables and assessment of optimized MEs

Selection of the optimized formulae for both Jas and Joj systems was based on that the droplet size and the PDI should be minimized while the viscosity could be in range. The optimized formula for Jas-ME was composed of 17.68% Jas, 13.93% water, and 68.40% surfactant mixtures (17.1% Span 80, 17.1% Tween 80, and 34.2% Labrasol). While the Joj-ME included 20.62% Joj, 15.58% water, and 63.80% surfactant mixtures (15.95% Span 80, 15.95% Tween 80, and 31.9% Labrasol). Tables 3 and 4 show the responses of the two optimized formulae for both Jas-ME-Opt and Joj-ME-Opt, respectively. As seen from the table a small acceptable residual error was obtained indicating the validity of the model for the preparation of MEs. The two selected formulae were investigated for further studies.

3.5.1. Morphological evaluation

The TEM images of the two optimized Jas-ME-Opt and Joj-ME-Opt formulations demonstrated spherical-shaped particles similar to those attained by other authors (Nasr and Abdel-Hamid, 2016; Yehia et al., 2017) as shown in Fig. 6. The average particle sizes obtained from DLS were concurring with those obtained using the TEM imaging technique.

3.5.2. Ex vivo skin deposition studies

Fig. 7 shows the skin deposition of the selected ME formulations in each skin layer, stratum corneum, epidermis, and dermis, in addition to the permeation into the receptor compartment measured over 24 h. TZR concentration was measured using a UV spectrophotometer at λ_{max} 347 nm compared to a blank to avoid any interference. By looking at the data of the control solutions, it was detected that only 2% of TZR was deposited onto the stratum corneum and 1.3% in the epidermis in the case of Jas with no detected drug in the case of Joj in both layers. In addition, no drug was noticed in the dermis and receptor compartment, in both Jas or Joj solutions, indicating the inability of TZR to permeate through the skin. On the other hand, it was clear that TZR was successfully deposited in the skin in both selected formulations. This could be attributed to TZR's high lipophilicity, allowing its solubilization in the oily phase and thus, effectively partitioned from the ME to the lipids

Table 3
Predicted, observed, and residual error values of the responses of the Jas-ME optimized formula.

Jas-ME-Opt				
Results	Droplet size (nm)	PDI	Viscosity (cP)	Conductivity (μS/cm)
Predicted values	11.03	0.19	299.65	
Actual values	11.71	0.18	300.00	9.57
Residual error %	94.25	104.89	99.89	

Abbreviations: Jas-ME-Opt; Jasmine oil microemulsion optimized formula, PDI; polydispersity index.
*Residual = predicted/actual*100.

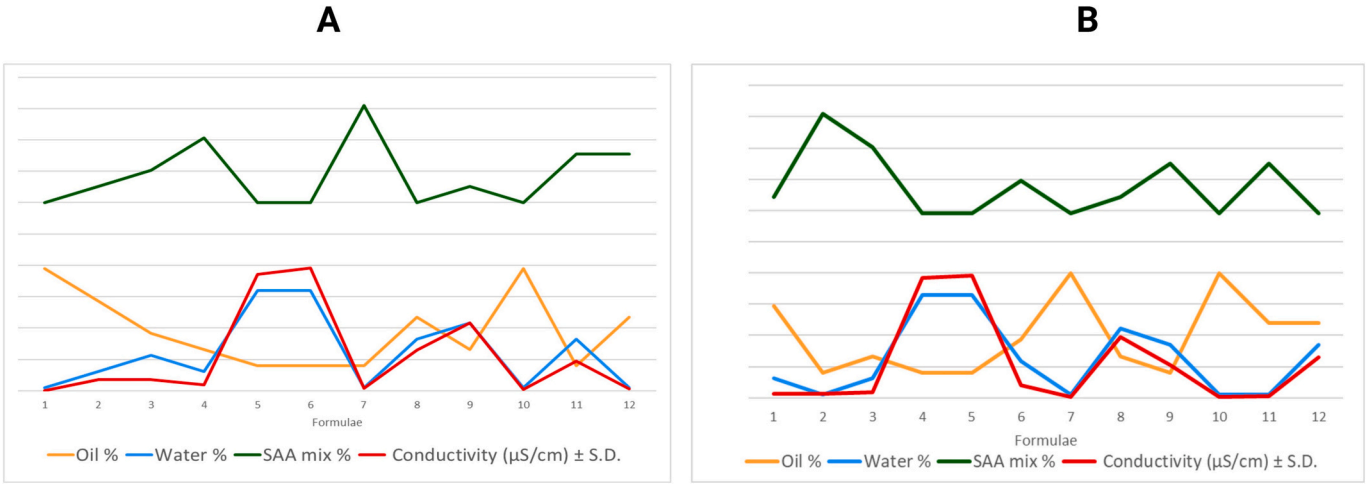

Fig. 5. Correlation between the conductivity values of the prepared MEs and the ME constituents (oil, water, and SAA mixtures percents): (A) Jas systems, (B) Joj systems.

Table 4
Predicted, observed, and residual error values of the responses of the Joj-ME optimized formula.

Joj-ME-Opt				
Results	Droplet size (nm)	PDI	Viscosity (cP)	Conductivity (μS/cm)
Predicted values	19.98	0.31	545.60	
Actual values	20.87	0.31	550.00	8.15
Residual error %	95.76	99.06	99.20	

Abbreviations: Joj-ME-Opt; Jojoba oil microemulsion optimized formula, PDI; polydispersity index.
*Residual = predicted/actual*100.

of the stratum corneum (Nasr et al., 2017). Moreover, the improved TZR skin deposition with our MEs could be due to the nanoscale size of the formulations and the permeation-enhancing properties of the surfactant and cosurfactant used and this was not the case in the oil solutions which were free from the merits of the ME nanosize and permeation enhancing characteristics (Nasr et al., 2017). ME also increases the skin retention of drugs, due to its lipophilic nature, which permits partitioning into the lipid layers of the skin, accumulating in the upper layers and acting as a depot which contributed to a more localized action (Lamie et al., 2022; Lopes, 2014).

Additionally, while studying the effect of formulation composition on TZR skin deposition, it was detected that the presence of the Jas and Joj, which are lipid complex mixtures, allow them to interact with the skin resulting in an enhanced penetration (Nawaz et al., 2022). EOs reversibly change the stratum corneum's lipid structure which eventually leads to the development of pores in the skin. As a result, the amount of drug that permeates the skin increases (Nawaz et al., 2022).

Interestingly, the Jas-ME-Opt formula displayed the highest performance, achieving a significant TZR deposition in all skin layers more than the Joj-ME-Opt formula. This could be ascribed to the increase in the degree of lipophilicity for Jas over the Joj as stated before which permits more solubilization in the oily phase for our hydrophobic drug. Thus, the drug will be successfully transferred to the stratum corneum's lipids from the ME (Nasr et al., 2017). Furthermore, this could be due to the higher viscosity of the Joj-ME-Opt selected formulation than the Jas-ME-Opt one which led to a reduced drug deposition (Nasr and Abdel-Hamid, 2016). It is also important to mention that both selected MEs displayed a small amount of permeated TZR in the receptor compartment suggesting that TZR formulations were delivered topically rather than transdermally due to their limited systemic distribution, which highlights their suitability for the treatment of acne.

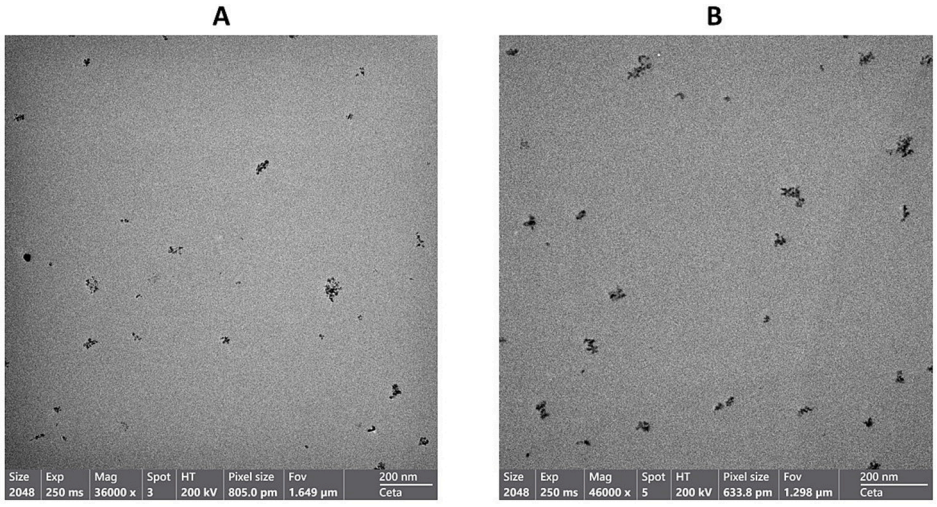

Fig. 6. TEM images for (A) Jas-ME-Opt, (B) Joj-ME-Opt formulations.

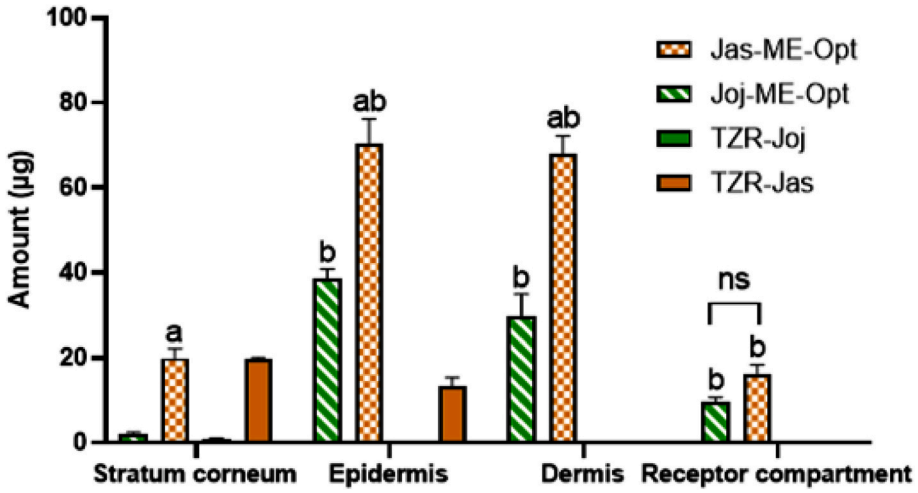

Fig. 7. *Ex vivo* skin deposition and distribution of TZR in the skin layers and receptor compartment after 24 h application of both the optimized formulae (Joj-ME-Opt & Jas-ME-Opt) and TZR oils solutions (TZR in Jas and TZR in Joj).
Results were compared using Two-way ANOVA followed by Sidak's *post hoc* test. a: $p < 0.0001$ compared with respective TZR deposited from Joj-ME-Opt. b: $p < 0.0001$ compared with respective TZR deposited from oil solution.

3.5.3. Qualitative tracing of the fluorescently labeled selected MEs using confocal laser scanning microscopy (CLSM)

Providing more evidence for previous results, accumulation and penetration extent in the skin layers of the fluorescently labeled TZR selected MEs were visualized. In this aspect, the lipophilic Dil fluorescent marker (log $P = 20$) was selected because it mimics the lipophilic TZR in the optimized MEs. Fig. 8A illustrated normal skin to ensure that no auto-fluorescence occurred, while Fig. 8B and C demonstrated the relative fluorescence intensity along with the depth of Dil fluorescent dye within the skin layers of the applied fluorescently Dil labeled MEs for 24 h.

It was obvious that the Dil-labeled selected MEs mostly accumulated in the deeper skin epidermis layer. The calculated intensities in the stratum corneum from Jas-ME-Opt and Joj-ME-Opt formulae were 30.21 $\pm$ 2.4 pixel/μm^2 and 15.31 $\pm$ 2.2 pixel/μm^2, respectively. Nevertheless, the fluorescence was intensified with high significance by application of Dil labeled Jas-ME-Opt (70.2 $\pm$ 3.7 pixel/μm^2, 65.1 $\pm$ 4.2 pixel/μm^2) over the Dil labeled Joj-ME-Opt formula (20.2 $\pm$ 4.1 pixel/μm^2, 10.4 $\pm$ 2.4 pixel/μm^2) in both epidermal and dermal layers, respectively. It was noticeable that the fluorescence in all layers from Jas-ME-Opt was significantly higher than that from Joj-ME-Opt p-value <0.0001.

These outcomes are consistent with those of the quantitative skin deposition tests, which reflects the superiority of the Jas-ME-Opt in penetrating the stratum corneum with minimal delay in the drug delivery into the deeper skin layers, confirming its capability in accumulating the drug moiety within the epidermal and dermal layers. This also suggested that the ME carrier followed the transfollicular pathway which is a transport *via* hair follicles by bypassing the stratum corneum barrier to the dermis (Subongkot et al., 2022), thus, it was evident that accumulation occurred in the hair follicles. Worth noting that, follicular targeting could be a remarkable selection to treat acne vulgaris (Ghasemiyeh and Mohammadi-Samani, 2020).

3.6. Antimicrobial activity assay

In the current investigation, the antimicrobial potential of TZR alone and in ME formulations was inspected. The minimum inhibitory concentrations (MIC) of TZR alone, Jas-ME-Opt, and Joj-ME-Opt selected formulae were evaluated against *P. acnes*. It was noticed that, TZR's primary mode of action for treating acne is through targeting the RAR receptors rather than owing an antibacterial activity. The results confirmed that TZR didn't show any inhibitory action against the *P. acnes* bacteria. On the other hand, both formulations showed antimicrobial activities with MIC of 3.125 $\pm$ 0.03 µL and 0.78 $\pm$ 0.01 µL for Jas-ME-Opt and Joj-ME-Opt, respectively. This may be attributed to the inclusion of Jas and Joj in the MEs that enhanced the formulation's antimicrobial effectiveness. It's worthy to note that, previous studies investigated the antibacterial activities of various EOs toward *P. acnes* and all were reported to possess notable antibacterial effects (Alzohairy, 2016; Wulansari et al., 2017; Zu et al., 2010). In particular, Jas and Joj have also been found to exhibit antibacterial activities against *P. acnes* (Al-Ghamdi et al., 2019; Gad et al., 2021; Masdar et al., 2022; Zu et al., 2010). Remarkably, the Joj-ME-Opt formulation showed improved antibacterial activity over the Jas-ME-Opt one which is presented in the form of a reduced MIC value and this result is in agreement with Zu et al. who studied the effect of ten essential oils against *P. acnes* and found that the least bactericidal activity was shown by the Jas (Zu et al., 2010). The Supplementary material: Fig. S2 shows the well plate of the antimicrobial activity study.

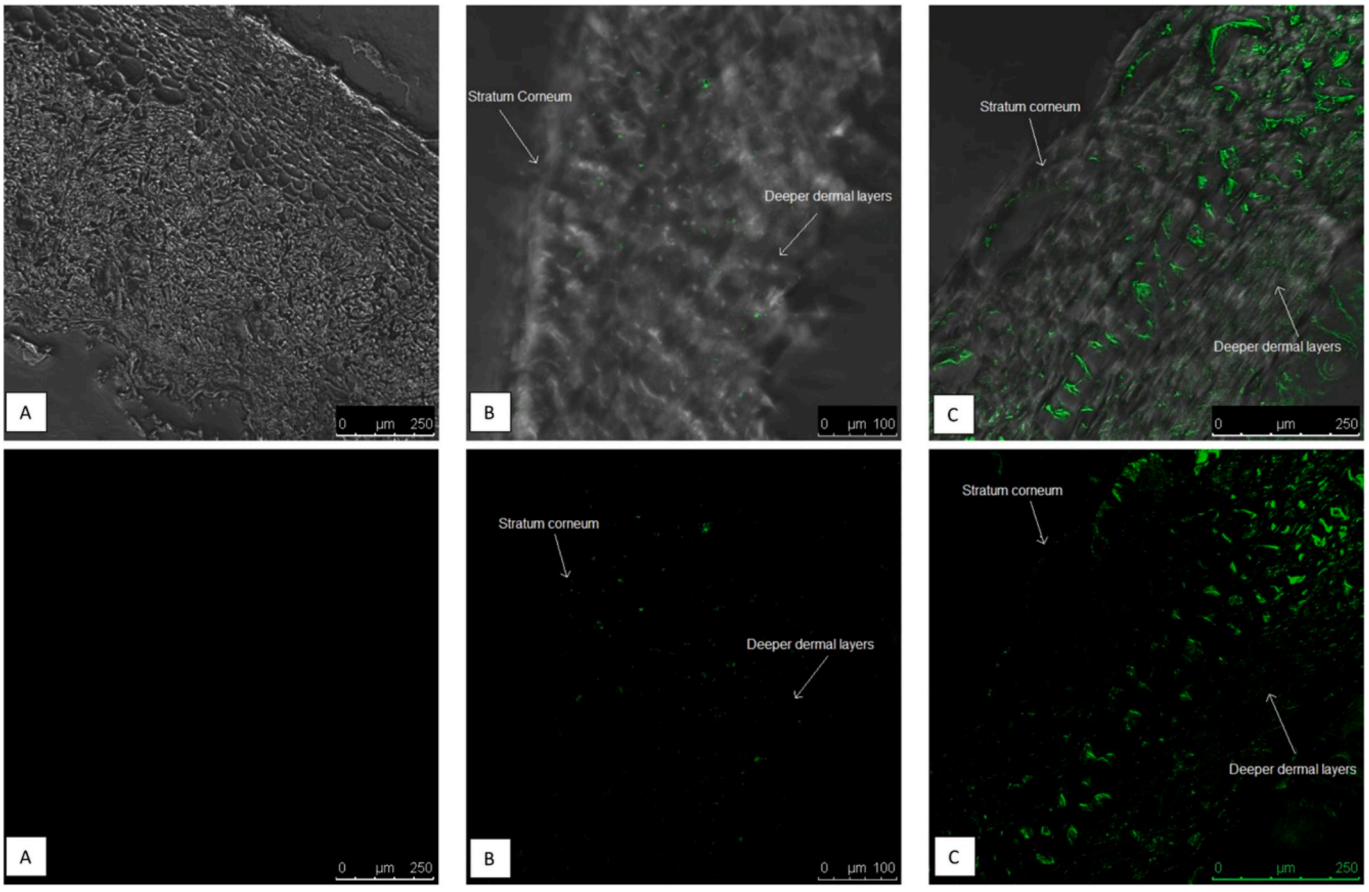

Fig. 8. CLSM images showing cross-sectional views of mice skin of (A) untreated skin, (B) skin treated with Joj-ME-Opt, (C) skin treated with Jas-ME-Opt after 24 h application.

3.7. In vivo study

3.7.1. Evaluation using acne mice model

P. acnes has been recognized as the main bacteria involved in the development of acne vulgaris pathogenesis in humans. Accordingly, *P. acnes* has been used to induce acne vulgaris in the auricles of different mouse strains, particularly Balb/c mice. When *P. acnes* is injected into the ears of mice, it induces inflammatory immune responses, resulting in the formation of microcomedones. In the current study, the microcomedone cysts were visually observed 24 h after an intradermal injection of living *P. acnes*. The left ear was left un-injected to serve as an uninfected control and was presumed to be group A (negative control group). The mice were then randomly divided into another four groups B, C, D & E. Group B received no treatment (model group), and Group C received the market product treatment (Zarotex gel). Groups D & E received the nominated treatments (Joj-ME-Opt and Jas-ME-Opt, respectively) which were initiated at Day 0. The therapy lasted for three consecutive days with a total of 5 doses of all the abovementioned treatments that were applied epicutaneously.

To track the changes, the difference in ear thickness was measured each day (Fig. 9) and photographed (Fig. 10). When compared to the normal (uninfected ears), it was obvious that the model group (B) acne, had a significant inflammatory response over the course of therapy which recorded the biggest increase in the average difference in ear thicknesses. This was further confirmed by the difference between the model ear and the normal ear as seen in the macrophotographs (Fig. 10A), where a definite cyst was evident along with swelling, redness, and erythema in the model ear (Fig. 10B). Moving on to the treatment groups, using the market product (Group C), there was not any significant reduction in the average difference in ear thickness from the model group (Fig. 10C). On the other hand, it was observed that as the course of the treatment progressed for Groups D & E, both ME formulations demonstrated a greater level of reduction in the average difference in ear thickness from the model group in just three days (Fig. 10D and E). It was detected that both Jas-ME-Opt and Joj-ME-Opt treated groups reached a high level of ear thickness reduction of 67.1% and 47.4%, respectively, while the market-treated group reached only 4%. According to these results, both ME selected formulations displayed a greater level of reduction than the market product. This could be clarified by the fact that TZR is known for its ability to treat acne disease; however, the available market product was in free form, which has a low deposition within the skin layers and necessitates a prolonged period of treatment to achieve the best results. While in the case of using both selected formulations, better results were achieved due to the ME effect as they display suitable skin permeation rates and skin uptake (Andrýsková et al., 2021). Thus, showing improved delivery of the drug into the deeper skin layers as mentioned earlier and hence demonstrating its capacity to accumulate the drug moiety inside the epidermal and dermal layers. Additionally, it was revealed that the ME has an ability to deposit TZR in the hair follicles, a key structure and promotor of acne development (Ghasemiyeh and Mohammadi-Samani, 2020; Subongkot et al., 2022).

Although both ME formulations groups showed significant differences from the model group, the magnitude of the significance of group E was much greater than that of group D, in which group E which was treated with Jas-ME-Opt showed a significant level of reduction in the average difference in ear thickness from the model group with $p < 0.005$ while that of Joj-ME-Opt showed a significant difference with $p < 0.05$, indicating the superiority of Jas-ME-Opt in the treatment of acne which is due to the greater ability of the Jas-ME-Opt to penetrate the stratum corneum and transport TZR to deeper layers of skin. This result is in agreement with the abovementioned better outcomes of the Jas-ME-Opt formula, in which it showed lower droplet size with less PDI value and lower viscosity along with improved *ex vivo* deposition among the skin layers, over the Joj-ME-Opt one.

3.7.2. Histopathological evaluation

After the treatment period, all mice were mercifully sacrificed and their ears were dissected for histopathological examination, which was based on the condition of the skin architecture, epidermal layer integrity, and dermal layer thickness, as well as the presence or absence of inflammatory cells and the state of the blood vessels. Fig. 11A showed the histological images of the normal ear (group A) revealed a typical arrangement of histological structures of different skin layers with a thin outer epidermal layer, intact well-ordered keratinocytes with intact subcellular details (arrow), and an integral dermal layer (star) with minimal inflammatory cells and normal vasculatures and intact subcutaneous layer, and this confirmed that animals were in the normal case with no evidence of inflammation prior to the study. On the other hand, the model ear (Fig. 11B) exhibited all the inflammatory signs of severe dermatitis with focal patches of epidermal necrosis and ulceration covered by necrotic tissue depress (arrow), as well as apparent intense inflammatory cells infiltrations causing edema and thickening of the whole layer (star). In addition, the visible congestion and dilation of subcutaneous blood vessels with hemorrhagic patches (red arrow), proved the success of our animal model. Furthermore, the histopathological examination of group C treated with the market product (Fig. 11C) showed almost the same records as model samples along with the insignificant improvement when compared to the model samples and this result is in good agreement with the evaluation of the ear

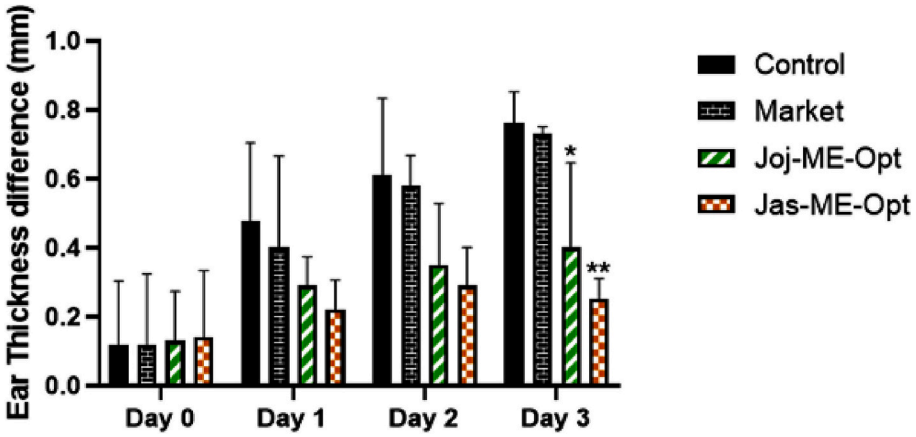

Fig. 9. Bar charts showing ear thickness difference at days 0, 1, 2, and 3 for the control (normal) group, market product group, Joj-ME-Opt treated group, and Jas-ME-Opt treated group.
* $P < 0.05$, ** $P < 0.005$.

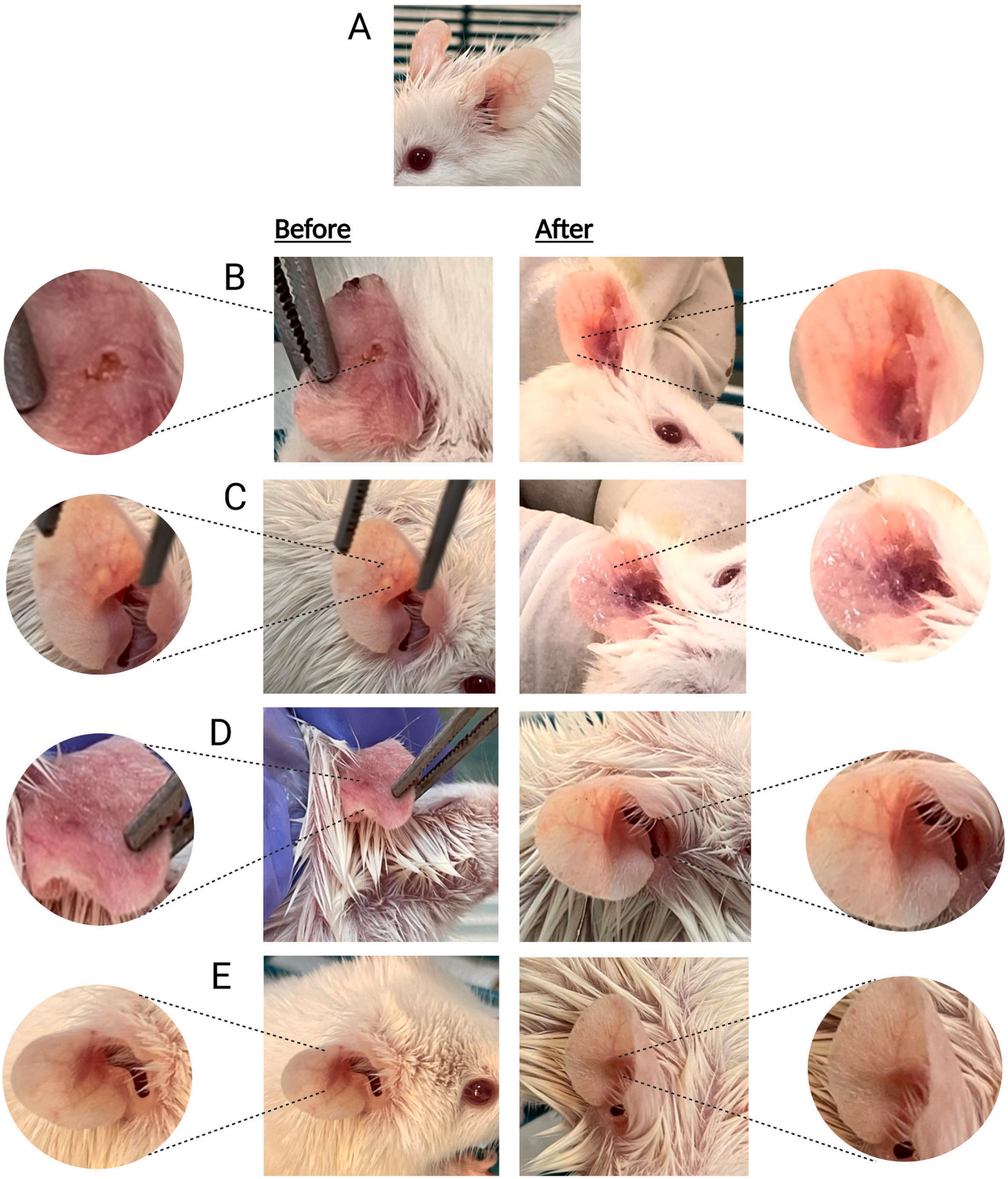

Fig. 10. Representative images of the infected ear acne mice model before and after treatment of (A) control (normal) group, (B) model (untreated) group, (C) group treated with the market product, (D) group treated with Joj-ME-Opt, and (E) group treated with Jas-ME-Opt.

thickness difference. The severe inflammatory cells (star), with hemorrhagic areas (red arrow), in addition to the necrotic tissue, depress (arrow) associated with the market group could be the result of prompting the TZR-related side effects such as redness, erythema, and dryness. It is noteworthy that skin irritation (erythema) is one of the main side effects of TZR therapy, which severely restricts its effectiveness and patients' acceptance (Patel et al., 2016). Also, it may be due to that the skin faced a high concentration of TZR at one time with any controlled release manner which may worsen the case.

On the other hand, samples from group D treated with Joj-ME-Opt

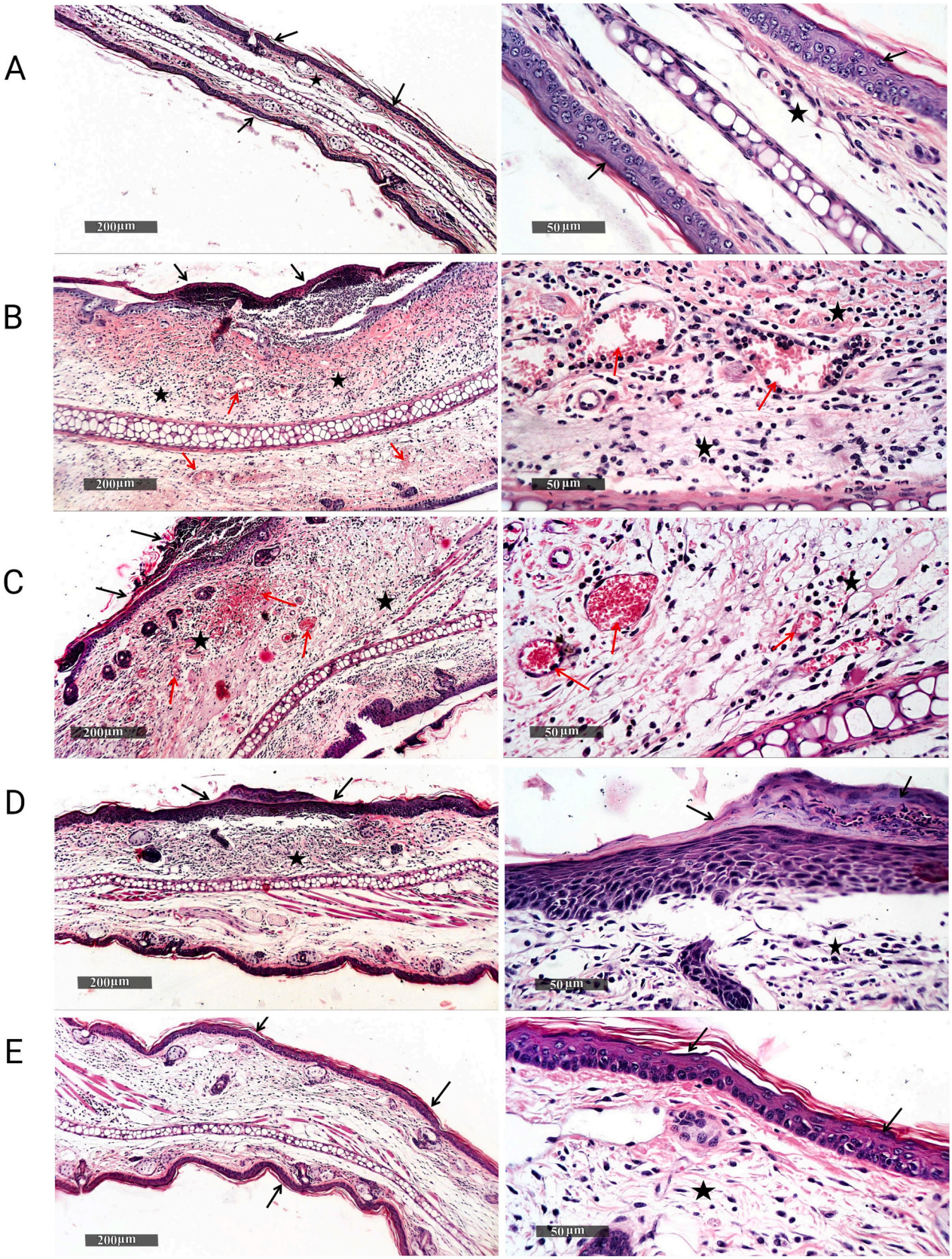

Fig. 11. Histopathological photomicrographs of H&E-stained infected ear sections of different animal groups: (A) control (normal) group, (B) model (untreated) group, (C) group treated with the market product, (D) group treated with Joj-ME-Opt, and (E) group treated with Jas-ME-Opt. Magnification power 200× and 50 × .

(Fig. 11D) showed significant protective and healing efficacy with a significant reduction of inflammatory reaction and inflammatory cell density in the dermal layer (star). Complete epidermal re-epithelialization with persistent epidermal thickening was noticed under small focal areas of necrotic tissue depression (arrow). Moreover, group E samples treated with Jas-ME-Opt (Fig. 11E) demonstrated the best protective efficacy with a more accelerated healing process compared to other treatment groups. Significant decreases of whole auricular thickness as well as epidermal thickness (arrow) were shown in addition to evident minimal dermal inflammatory cell infiltrates records (star) which were observed when compared to model samples. This superiority in the results for groups D and E over the market group could be ascribed to the ME enhancement effect. It was reported that most of the currently available conventional dosage forms, such as creams, lotions, and gels, are incapable of reducing the irritation caused by TZR topical application (Draize, 1944; Shah et al., 2007). Thereby, the encapsulation of TZR in ME is hypothesized to reduce skin irritation (Patel et al., 2016). While focusing on group E results which were better than group D, this could be explained by the enhanced skin retention and thus, higher therapeutic effect for the Jas-ME-Opt over the Joj-ME-Opt as discussed before.

It's important to mention that, although Joj-ME-Opt showed an enhanced antibacterial effect over the Jas-ME-Opt but the latter revealed a better skin deposition that resulted in effective topical TZR delivery and thus showed improved therapeutic effect. All of these findings strongly suggest that Jas-ME-Opt has a remarkable ability to deliver TZR topically and to treat acne successfully.

4. Conclusion

In the current study, TZR-loaded EO-MEs were successfully prepared using either Jas or Joj. The selected formulations using either Jas-ME-Opt or Joj-ME-Opt exhibited acceptable characteristics in terms of droplet size, PDI, viscosity, electrical conductivity as well as vesicular morphology. In addition, the droplet nanosize of the MEs and the proper choice of components were the two main factors that considerably improved therapeutic efficacy, and decreased the risk for irritation of TZR when compared *in vivo* to the conventionally marketed formulation. It is remarkable that, although Joj-ME-Opt showed augmented antibacterial activity against *P. acnes* over the Jas-ME-Opt, other results confirmed that the optimized Jas-ME-Opt showed significant superiority over the Joj-ME-Opt in the *ex vivo* skin retention that was reflected in the outcomes of the *in vivo* investigation. Therefore, Jas-ME-Opt could be considered an auspicious carrier system for TZR topical delivery in mitigating acne vulgaris symptoms.

CRediT authorship contribution statement

Noha M. Badawi: Writing – original draft, Writing – review & editing, Data curation, Visualization, Investigation, Validation. **Rania M. Yehia:** Methodology, Visualization, Conceptualization, Investigation, Validation, Resources. **Caroline Lamie:** Visualization, Investigation, Methodology, Validation. **Khaled A. Abdelrahman:** Methodology, Visualization, Investigation, Resources. **Dalia A. Attia:** Conceptualization, Supervision, Visualization, Investigation, Project administration, Writing – review & editing, Data curation. **Doaa A. Helal:** Writing – original draft, Investigation, Data curation.

Declaration of Competing Interest

The authors declare that they have no known competing financial interests or personal relationships that could have appeared to influence the work reported in this paper.

Data availability

The datasets generated or analyzed during the current study are available from the corresponding author upon reasonable request.

Acknowledgment

The authors are thankful to 5th-year students of the Pharmaceutics Research Methodology Module at the Faculty of Pharmacy, The British University in Egypt; Ahmed Ibrahim, Hussam Mohamed, Mariam Mostafa, Mostafa Sabry, Raneem Ahmed, Raneem Salah, Roaa Sami, and Rawan Tarek, for their cooperation and participation in the practical part of this work.

Appendix A. Supplementary data

Supplementary data to this article can be found online at https://doi.org/10.1016/j.ijpx.2023.100185.

References

Abdelhamed, F.M., Abdeltawab, N.F., ElRakaiby, M.T., Shamma, R.N., Moneib, N.A., 2022. Antibacterial and anti-inflammatory activities of *Thymus vulgaris* essential oil nanoemulsion on acne vulgaris. Microorganisms 10, 1874.
Al-Ghamdi, A., Elkholy, T., Abuhelal, S., Al-Abbadi, H., Qahwaji, D., Khalefah, N., Sobhy, H., Abu-Hilal, M., 2019. Antibacterial and antifungal activity of jojoba wax liquid (*Simmondsia chinensis*). Pharmacogn. J. 11.
Alzohairy, M.A., 2016. Therapeutics role of *Azadirachta indica* (Neem) and their active constituents in diseases prevention and treatment. Evid. Based Complementary Altern. Med. 2016.
Andrýsková, N., Sourivong, P., Babincová, M., Šimaljaková, M., 2021. Controlled release of tazarotene from magnetically responsive nanofiber patch: towards more efficient topical therapy of psoriasis. Appl. Sci. 11, 11022.
Bachhav, Y.G., Patravale, V.B., 2009. Microemulsion based vaginal gel of fluconazole: formulation, in vitro and in vivo evaluation. Int. J. Pharmaceut. 365, 175–179.
Butt, U., ElShaer, A., Snyder, L.A., Chaidemenou, A., Alany, R.G., 2016. Fatty acid microemulsion for the treatment of neonatal conjunctivitis: quantification, characterisation and evaluation of antimicrobial activity. Drug Deliv. Transl. Res. 6, 722–734.
Das, S., Gupta, K.S., 2021. A comprehensive review on natural products as chemical penetration enhancer. J. Drug Deliv. Ther. 11, 176–187.
Djordjevic, L., Primorac, M., Stupar, M., Krajisnik, D., 2004. Characterization of caprylocaproyl macrogolglycerides based microemulsion drug delivery vehicles for an amphiphilic drug. Int. J. Pharmaceut. 271, 11–19.
Draize, J.H., 1944. Methods for the study of irritation and toxicity of substances applied topically to the skin and mucous membranes. J. Pharmacol. Exp. Ther. 82, 377–390.
Duangjit, S., Mehr, L.M., Kumpugdee-Vollrath, M., Ngawhirunpat, T., 2014. Role of simplex lattice statistical design in the formulation and optimization of microemulsions for transdermal delivery. Biol. Pharm. Bull. b14–00549.
Figueiredo, A.C., 2017. Biological properties of essential oils and volatiles: sources of variability. Nat. Volatiles Essent. Oils 4, 1–13.
Fox, L.T., Gerber, M., Plessis, J.D., Hamman, J.H., 2011. Transdermal drug delivery enhancement by compounds of natural origin. Molecules 16, 10507–10540.
Fox, L., Csongradi, C., Aucamp, M., Du Plessis, J., Gerber, M., 2016. Treatment modalities for acne. Molecules 21, 1063.
Gad, H.A., Roberts, A., Hamzi, S.H., Gad, H.A., Touiss, I., Altyar, A.E., Kensara, O.A., Ashour, M.L., 2021. Jojoba oil: an updated comprehensive review on chemistry, pharmaceutical uses, and toxicity. Polymers 13, 1711.
Ghasemiyeh, P., Mohammadi-Samani, S., 2020. Potential of nanoparticles as permeation enhancers and targeted delivery options for skin: advantages and disadvantages. Drug Des. Devel. Ther. 14, 3271.
Gregoriou, S., Kritsotaki, E., Katoulis, A., Rigopoulos, D., 2014. Use of tazarotene foam for the treatment of acne vulgaris. Clin. Cosmet. Investig. Dermatol. 7, 165.
Hashem, F.M., Shaker, D.S., Ghorab, M.K., Nasr, M., Ismail, A., 2011. Formulation, characterization, and clinical evaluation of microemulsion containing clotrimazole for topical delivery. AAPS PharmSciTech 12, 879–886.
Hathout, R.M., Elshafeey, A.H., 2012. Development and characterization of colloidal soft nano-carriers for transdermal delivery and bioavailability enhancement of an angiotensin II receptor blocker. Eur. J. Pharm. Biopharm. 82, 230–240.
Hathout, R.M., Woodman, T.J., Mansour, S., Mortada, N.D., Geneidi, A.S., Guy, R.H., 2010. Microemulsion formulations for the transdermal delivery of testosterone. Eur. J. Pharm. Sci. 40, 188–196.
Herman, A., Herman, A.P., 2015. Essential oils and their constituents as skin penetration enhancer for transdermal drug delivery: a review. J. Pharm. Pharmacol. 67, 473–485.
Katsambas, A., Dessinioti, C., 2008. New and emerging treatments in dermatology: acne. Dermatol. Ther. 21, 86–95.
Khichariya, A., Jeswani, G., Choudhary, R., Alexander, A., Nakhate, K.T., Badwaik, H.R., 2022. Formulation of plumbagin-loaded microemulsion: evaluation of anti-rheumatoid efficacy in Wistar rat model. J. Mol. Liq. 363, 119851.

Kizibash, N.A., Shah, S.S., Alenizi, D., Nazar, M.F., Asif, S., 2011. Design of a microemulsion-based drug delivery system for diclofenac sodium. J. Chem. Soc. Pak. 33, 1.
Lamie, C., Elmowafy, E., Attia, D.A., Elmazar, M.M., Mortada, N.D., 2022. Diversifying the skin cancer-fighting worthwhile frontiers: how relevant are the itraconazole/ascorbyl palmitate nanovectors? Nanomed. Nanotechnol. Biol. Med. 43, 102561.
Lawrence, M.J., Rees, G.D., 2000. Microemulsion-based media as novel drug delivery systems. Adv. Drug Deliv. Rev. 45, 89–121.
León-Méndez, G., Pájaro-Castro, N., Pájaro-Castro, E., Torrenegra-Alarcón, M., Herrera-Barros, A., 2019. Essential oils as a source of bioactive molecules. Revista Colombiana de Ciencias Químico-Farmacéuticas 48, 80–93.
Lopes, L.B., 2014. Overcoming the cutaneous barrier with microemulsions. Pharmaceutics 6, 52–77.
Luo, J., He, W., Li, X., Ji, X., Liu, J., 2021. Anti-acne vulgaris effects of chlorogenic acid by anti-inflammatory activity and lipogenesis inhibition. Exp. Dermatol. 30, 865–871.
Masdar, N.D., Uyup, N.H., Zainol, Z.E., Roslani, M.A., Anuar, S.N.S., Zulkafle, M.A., 2022. The chemical properties and anti-acne activity determination of *Swietenia macrophylla* seed extracts. Malays. J. Anal. Sci. 26, 229–240.
Mazonde, P., Khamanga, S.M., Walker, R.B., 2020. Design, optimization, manufacture and characterization of Efavirenz-loaded flaxseed oil nanoemulsions. Pharmaceutics 12, 797.
Mohiuddin, A., 2019. Acne protection: measures and miseries. Dermatol. Clin. Res. 5, 272–311.
Morais, G.G., Santos, O.D., Oliveira, W.P., Filho, P.A.R., 2008. Attainment of O/W emulsions containing liquid crystal from annatto oil (*Bixa orellana*), coffee oil, and tea tree oil (Melaleuca alternifolia) as oily phase using HLB system and ternary phase diagram. J. Dispers. Sci. Technol. 29, 297–306.
Nasr, M., Abdel-Hamid, S., 2016. Optimizing the dermal accumulation of a tazarotene microemulsion using skin deposition modeling. Drug Dev. Ind. Pharm. 42, 636–643.
Nasr, M., Abdel-Hamid, S., Moftah, N.H., Fadel, M., Alyoussef, A.A., 2017. Jojoba oil soft colloidal nanocarrier of a synthetic retinoid: preparation, characterization and clinical efficacy in psoriatic patients. Curr. Drug Deliv. 14, 426–432.
Nastiti, C.M., Ponto, T., Abd, E., Grice, J.E., Benson, H.A., Roberts, M.S., 2017. Topical nano and microemulsions for skin delivery. Pharmaceutics 9, 37.
Nawaz, A., Farid, A., Safdar, M., Latif, M.S., Ghazanfar, S., Akhtar, N., Al Jaouni, S.K., Selim, S., Khan, M.W., 2022. Formulation development and ex-vivo permeability of curcumin hydrogels under the influence of natural chemical enhancers. Gels 8, 384.
Nazzaro, F., Fratianni, F., Coppola, R., De Feo, V., 2017. Essential oils and antifungal activity. Pharmaceuticals 10, 86.
Otlewska, A., Baran, W., Batycka-Baran, A., 2020. Adverse events related to topical drug treatments for acne vulgaris. Expert Opin. Drug Saf. 19, 513–521.
Patel, M.R., Patel, R.B., Parikh, J.R., Patel, B.G., 2016. Novel microemulsion-based gel formulation of tazarotene for therapy of acne. Pharm. Dev. Technol. 21, 921–932.
Putri, F.L.A., Nugroho, A.K., Setyowati, E.P., 2018. Optimization of HIB value combination of tween 60 and span 80 on cream formulation of ethanol extract of green tea leaves (*Camellia Sinensis* L.). Majalah Obat Tradisional 23, 124–130.
Radwan, S.A.A., ElMeshad, A.N., Shoukri, R.A., 2017. Microemulsion loaded hydrogel as a promising vehicle for dermal delivery of the antifungal sertaconazole: design, optimization and ex vivo evaluation. Drug Dev. Ind. Pharm. 43, 1351–1365.
Rodríguez-Rojo, S., Varona, S., Núñez, M., Cocero, M., 2012. Characterization of rosemary essential oil for biodegradable emulsions. Ind. Crop. Prod. 37, 137–140.
Sarheed, O., Dibi, M., Ramesh, K.V., 2020. Studies on the effect of oil and surfactant on the formation of alginate-based O/W lidocaine nanocarriers using nanoemulsion template. Pharmaceutics 12, 1223.
Sevimli Dikicier, B., 2019. Topical treatment of acne vulgaris: efficiency, side effects, and adherence rate. J. Int. Med. Res. 47, 2987–2992.
Shah, K.A., Date, A.A., Joshi, M.D., Patravale, V.B., 2007. Solid lipid nanoparticles (SLN) of tretinoin: potential in topical delivery. Int. J. Pharmaceut. 345, 163–171.
Shevachman, M., Shani, A., Garti, N., 2004. Formation and investigation of microemulsions based on jojoba oil and nonionic surfactants. J. Am. Oil Chem. Soc. 81, 1143–1152.
Subongkot, T., Ngawhirunpat, T., 2017. Development of a novel microemulsion for oral absorption enhancement of all-trans retinoic acid. Int. J. Nanomedicine 12, 5585.
Subongkot, T., Charernsriwilaiwat, N., Chanasongkram, R., Rittem, K., Ngawhirunpat, T., Opanasopit, P., 2022. Development and skin penetration pathway evaluation using confocal laser scanning microscopy of microemulsions for dermal delivery enhancement of finasteride. Pharmaceutics 14, 2784.
Taylor, M., Gonzalez, M., Porter, R., 2011. Pathways to inflammation: acne pathophysiology. Eur. J. Dermatol. 21, 323–333.
Thombre, N.A., Niphade, P.S., Ahire, E.D., Kshirsagar, S.J., 2022. Formulation development and evaluation of microemulsion based lornoxicam gel. Biosci. Biotechnol. Res. Asia 19, 69–80.
Vlaia, L., Olariu, I., Muț, A.M., Coneac, G., Vlaia, V., Anghel, D.F., Maxim, M.E., Stângă, G., Dobrescu, A., Suciu, M., 2022. New, biocompatible, chitosan-gelled microemulsions based on essential oils and sucrose esters as nanocarriers for topical delivery of fluconazole. Pharmaceutics 14, 75.
Vostinaru, O., Heghes, S.C., Filip, L., 2020. Safety profile of essential oils. In: Essential Oils-Bioactive Compounds, New Perspectives and Applications, pp. 1–13.
Williams, H.C., Dellavalle, R.P., Garner, S., 2012. Acne vulgaris. Lancet 379, 361–372.
Wulansari, A., Jufri, M., Budianti, A., 2017. Studies on the formulation, physical stability, and in vitro antibacterial activity of tea tree oil (Melaleuca alternifolia) nanoemulsion gel. Int. J. Appl. Pharmaceut. 9, 135–139.
Yehia, R., Attia, D.A., 2019. The microemulsion as a key player in conquering the skin barrier for the aim of transdermal delivery of drugs: reviewing a successful decade. Asian J. Pharm. Clin. Res. 12, 34–48.
Yehia, R., Hathout, R.M., Attia, D.A., Elmazar, M.M., Mortada, N.D., 2017. Anti-tumor efficacy of an integrated methyl dihydrojasmonate transdermal microemulsion system targeting breast cancer cells: in vitro and in vivo studies. Colloids Surf. B: Biointerfaces 155, 512–521.
Yehia, R.M., Attia, D.A., Elmazar, M.M., El-Nabarawi, M.A., Teaima, M.H., 2022. Screening of adapalene microsponges fabrication parameters with insight on the in vitro biological effectiveness. Drug Des. Devel. Ther. 3847–3864.
Yuliani, S., Noveriza, R., 2019. Effect of carrier oil and co-solvent on the formation of clove oil nanoemulsion by phase inversion technique. In: IOP Conference Series: Earth and Environmental Science. IOP Publishing, p. 012036.
Zu, Y., Yu, H., Liang, L., Fu, Y., Efferth, T., Liu, X., Wu, N., 2010. Activities of ten essential oils towards *Propionibacterium acnes* and PC-3, A-549 and MCF-7 cancer cells. Molecules 15, 3200–3210.